

A novel receptor for detection of Zn^{2+} metal ion and F^- , H_2PO_4^- and AcO^- anions in aqueous media: a DFT study

Masoumeh Orojloo¹ · Raziye Arabahmadi² · Fatemeh Naderi¹ · Fatemeh Parchegani¹ ·
Mohammad Solimannejad¹ · Peyman Zolgharnein³ · Saeid Amani¹

Received: 11 July 2017 / Accepted: 5 October 2017 / Published online: 9 October 2017
© Institute of Chemistry, Slovak Academy of Sciences 2017

Abstract A new colorimetric chemosensor **L**, containing electron-donating moieties attached to the thiazole-based Schiff base was synthesized. The optical and colorimetric sensing properties of **L** for anions and cations were investigated using naked eye, UV–Vis and computational studies. The receptor **L** displays visual changes towards anions like F^- , H_2PO_4^- and AcO^- and also towards cation such as Zn^{2+} in DMSO. Other anions such as Cl^- , Br^- , I^- , NO_3^- and HSO_4^- did not cause any color change. On the addition of other metal ions such as Cr^{3+} , Mn^{2+} , Fe^{3+} , Co^{2+} , Ni^{2+} , Cu^{2+} , Cd^{2+} , Hg^{2+} and Pb^{2+} , the receptor did not show any significant change. The binding constant (K_a) and stoichiometry of the host–guest complex formed were calculated by the Benesi–Hildebrand (B–H) plot and Job’s plot method,

respectively. Computational studies and UV–Vis titration were further used to emphasize the sensing behavior of the receptor. Quantum chemical calculations and molecular studies using Density Functional Theory and Molecular Electrostatic Potential surface studies were carried out to supplement the experimental results and gain deeper insights about the structural as well as the spectral aspects of the complex.

Graphical Abstract Receptor **L** proved to be a fluorescence and colorimetric Zn (II), fluoride (F^-), di-hydrogen phosphate (H_2PO_4^-) and acetate (AcO^-) sensor. This new chromogenic receptor shows a highly selective coloration for the above ions. The chemosensor showed a color change upon addition of Zn (II), or fluoride or di-hydrogen phosphate or acetate ions.

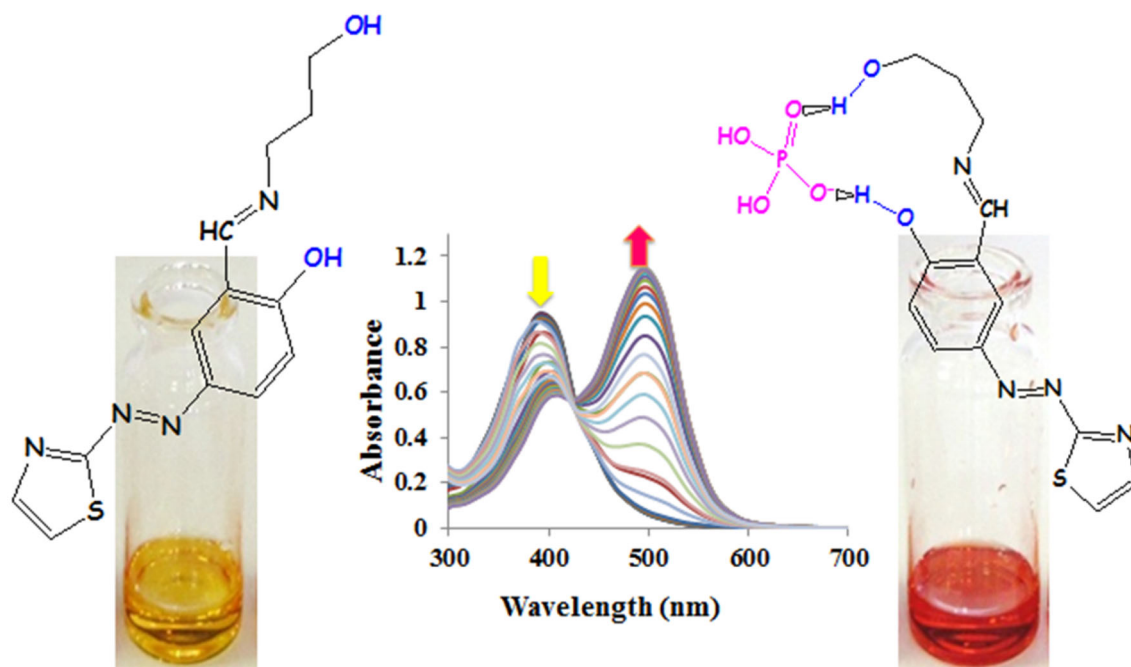
Electronic supplementary material The online version of this article (doi:10.1007/s11696-017-0312-7) contains supplementary material, which is available to authorized users.

✉ Saeid Amani
s-amani@araku.ac.ir

¹ Chemistry Department, Faculty of Sciences, Arak University, Dr. Beheshti Ave, Arak 38156-88349, Iran

² Chemistry Department, Payame Noor University (PNU), Tehran 19395-3697, Iran

³ Material Science and Engineering Department, The University of Sheffield, Sheffield, UK



Keywords Naked-eye detection · Chemosensor · DFT Calculations · Thiazole Schiff base

Introduction

Highly selective receptors are strongly preferred for practical applications. In reality, only a few examples of sensors capable of detecting particular ions both in organic and aqueous media have been simultaneously reported. On the other hand, the detection of multiple targets having a single receptor would be more efficient and also cost effective than a one-to-one analysis method, and so would attract more attention (Liu et al. 2013). The design of molecular probes, which is capable of recognizing metal ions and anions, is a welcoming development in the biological industry and environmental processes due its significant potential applications (Li et al. 2011, 2013; Tomat and Lippard 2010; Zyryanov et al. 2007; Kang et al. 2010; Hu et al. 2010; Yoon et al. 2006; Buccella et al. 2011; Xu et al. 2009; Xue et al. 2012; Jiang and Guo 2004). Anions such as H_2PO_4^- , F^- and AcO^- play vital role in the areas of biology, environmental hazard, medicine, catalysis among others; hence, its recognition and sensing have gained considerable interest (Beer and Gale 2001; Lavigne and Anslyn 2001; Martinez-Manez and Sancenón 2003, 2006; Sessler and Seidel 2003; Gunlaugsson et al. 2006; Gale et al. 2008; Santos-Figueroa et al. 2013). As the second most abundant transition metal in the human body after iron, Zn^{2+} is indispensable for mediating various enzyme-catalyzed reactions and therefore plays a crucial role in a

wide variety of physiological and pathological processes (Wang et al. 2011; Maret et al. 1999; Zalewski et al. 1993; Falchuk 1998). The growing importance of Zn^{2+} in neurological signaling and some proposed functions in biological systems have generated an urgent demand for the development of Zn^{2+} specific molecular probes (Frederickson et al. 2006; Berg and Shi 1996; Assaf and Chung 1984; Burdette and Lippard 2001, 2003). Moreover, the paramount and most important limitations for zinc detection result from the interference of other transition metal ions, especially cadmium (Safin et al. 2013). Therefore, it is worthwhile to pay attention to the development of sensors capable of detecting selectively zinc ions from cadmium.

Schiff bases are common organic structures which can be easily synthesized through a one-step synthetic procedure (Borisova et al. 2007; Vigato et al. 2007; Li et al. 2009; Lee et al. 2010; Sarkar et al. 2009; Cozzi 2004). Several heterocycles, especially thiazoles, occupy a key position owing to their versatile bioactivities due to the presence of multifunctional groups (Li et al. 2010, 2012, 2014; Venugopala and Jayashree 2003; Leung and MacLachlan 2007; Borisenko et al. 2006; Vashi and Naik 2004; Joseyphus et al. 2006; Chohan et al. 2004). Schiff bases from thiazole derived from salicylaldehyde derivatives are reported to have significant antibacterial, antifungal and anticancer activities (Orojloo et al. 2017). Based on these considerations in mind and our previous work (Orojloo and Amani 2016), herein, we report a novel colorimetric chemosensor **L** for recognition of Zn^{2+} metal ions and important biological anions. Receptor **L** can

detect Zn^{2+} by color change from yellow to orange via the ‘naked eye’ with high selectivity in DMSO environment. In addition, chromogenic receptor **L** possessing two phenolic and alcoholic OH, binds H_2PO_4^- , F^- and AcO^- via hydrogen bonding by fast response and excellent color change from yellow to red via naked-eye detection. The most difficult fact in the anion sensing in aqueous environment is that water is a highly competitive solvent and interferes with the detection process of anions by intervening in the interaction between associates (Orojloo and Amani 2017). To the best of our knowledge, this receptor is the first unsymmetrical thiazole-based colorimetric chemosensor use in qualitative and quantitative detection of biologically significant anions both in organic and aqueous media. Quantum chemical calculations and molecular studies using Density Functional Theory (DFT) and molecular electrostatic potential results surface (MEP) studies have been conducted to supplement the experimental results.

Materials and methods

General information

All the solvents and reagents (analytical and spectroscopic grade) that were used in this research were purchased from Sigma-Aldrich and Merck and used as received. Electronic spectral measurements were performed using Optizen 3220 UV spectrophotometer in the range of 200–900 nm at room temperature. $^1\text{H-NMR}$ spectra were recorded on Bruker AV 300 MHz and BrukerAvance III 400 MHz spectrometers, and chemical shifts were recorded in ppm. FT-IR spectra were recorded as pressed KBr discs, using Unicom Galaxy Series FT-IR 5000 spectrophotometer in the region of 400–4000 cm^{-1} . The matrix-assisted lasers desorption/ionization time-of-flight (MALDI-TOF) mass spectrometry was measured using a Bruker Reflex III spectrometer.

Synthesis of Azo-coupled salicylaldehyde precursor and receptor (**L**)

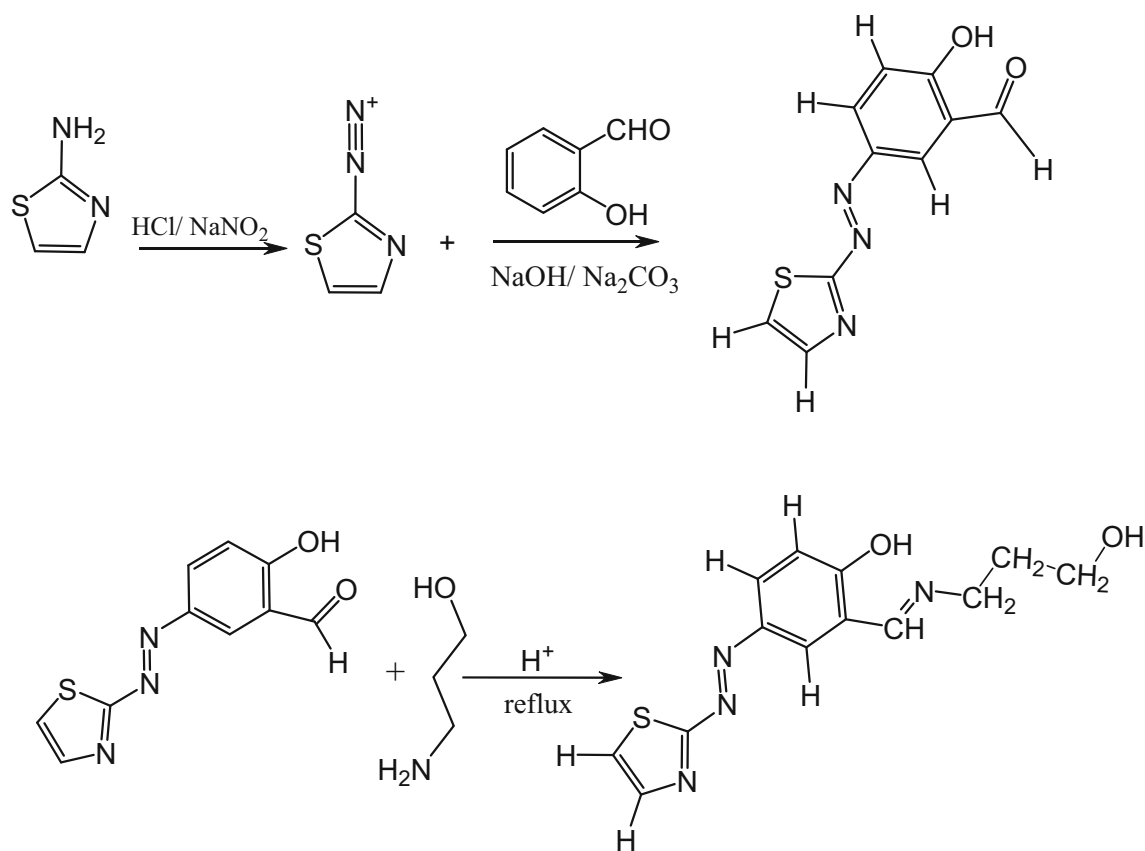
Azo-coupled salicylaldehyde precursor (2-hydroxy-5-(thiazol-2-ylidiazenyl)benzaldehyde) and 2-((E)-(3-hydroxypropylimino)methyl)-4-((E)-thiazol-2ylidiazenyl)phenol (receptor **L**), were synthesized and characterized according to our last published paper (Scheme 1) (Orojloo et al. 2017).

Results and discussion

Chromogenic Zn(II) sensing

The selectivity of receptor **L** toward various metal cations, viz., Cr^{3+} , Mn^{2+} , Fe^{3+} , Co^{2+} , Ni^{2+} , Cu^{2+} , Zn^{2+} , Cd^{2+} , Hg^{2+} and Pb^{2+} was primarily studied by UV–Vis spectroscopy in DMSO. Initially, we used the naked-eye colorimetric experiments to investigate the recognition ability of chemosensor **L** ($4 \times 10^{-5}\text{M}$) as chloride salt for the above-mentioned cation in DMSO. Upon the addition of 20 equivalent of the afore-mentioned metal cations to the solution of **L**, only Zn^{2+} caused a remarkable color changed from yellow to orange, while other metals caused no change in color in DMSO (Fig. 1a). The sensing behavior of sensor **L** towards Zn^{2+} was monitored by UV–Vis spectrophotometric method in DMSO. A solution of chemosensor **L** was titrated with increasing volume of concentrated solution of given cation. On incremental addition of Zn^{2+} to **L** in DMSO, the intensity of absorption band at 395 nm gradually decreased and a new absorption band at 495 nm was progressively formed resulting an isosbestic point at 410 nm (Fig. 1b). Notably, the large bathochromic shift, resulting from the extended ICT process, was responsible for a comprehensible color change from yellow to orange (Modi et al. 1970; Gentili 2007). The binding constant of complexation was calculated using the Benesi–Hildebrand method (Fig. S1). (Benesi and Hildebrand 1949) The resulting values are summarized in Table 1. For practical purposes, the detection limit of receptor **L** for the analysis of Zn^{2+} ion was also an important parameter (Lin et al. 2012). The detection limit of receptor **L** for the analysis of Zn^{2+} was calculated to be 48.9 μM which is comparable to various salicylaldimine Schiff base-type probes previously reported (Wang et al. 2015).

The conclusive stoichiometric ratio between (**L**) and Zn^{2+} was inferred to be 2:1 with the help of Job’s plot (Fig. S2) and molar ratio plot (inset of Fig. 1b) experiments (Likussar and Boltz 1971; Momoki et al. 1969). To validate the stoichiometry between the chemosensor **L** and Zn^{2+} ions, a MALDI-TOF mass examination was carried out (Fig. S3) (Orojloo et al. 2017). In this regard, the formation of 2:1 complex between **L** and Zn^{2+} was further confirmed by the appearance of peaks at m/z 643.0 corresponding to $[\text{2L} + \text{Zn(II)-1H}]^+$ mononuclear complex (calcd. 643.1) and 291.0 assignable to $[\text{L} + \text{H}]^+$ (calcd. 291.3 for $\text{C}_{13}\text{H}_{14}\text{N}_4\text{O}_2\text{S}$ formula), respectively. To illustrate more detailed information on the nature of binding mode of **L** with Zn^{2+} ions, FT-IR spectra of the sensor **L** and its Zn^{2+} complex were also measured (Fig. S4). The FT-IR spectrum of Zn^{2+} complex compared with that of free



Scheme 1 Synthesis of azo dye and receptor **L**

sensor **L** demonstrates that the $\nu(\text{C}=\text{N})$ band at 1629 cm^{-1} was red when shifted to lower frequency (from 1659 cm^{-1}). Reduction of the double bond character of the $\text{C}=\text{N}$ bond, which is caused by the coordination of nitrogen into the metal center, is in accordance with the results obtained from similar complexes (Shang et al. 2009; Prodi et al. 2011). Furthermore, meaningful changes were observed in the $\nu(\text{C}-\text{O})$ of phenolic band, expressing the involvement of the hydroxyl on the phenyl in the complexation of the receptor with the Zn^{2+} ion. Based on data from earlier reports, we could assign the bands at 482 and 542 cm^{-1} to $\text{Zn}-\text{N}$ and $\text{Zn}-\text{O}$ vibrations, respectively (Canpolat and Kaya 2005; Shen et al. 2008).

Also, we achieved $^1\text{H-NMR}$ experiment for more concrete evidence of the binding of the Zn^{2+} . As presented in Fig. S5a, the free ligand showed sharp peaks at 11.59, and 9.35 and within the range of 7.42–8.21 ppm corresponding to the phenolic OH, imine proton and aromatic peaks, respectively. Upon complexation with zinc ions, the adjacent peaks merged together, proving the structure of the complex inflexible as compared to the free ligand. In close insight, the phenolic proton signal at 11.59 ppm disappeared completely and the singlet associated with imine proton ($\text{CH}=\text{N}$) showed a clear up field shift by $\Delta\delta = -$

0.8 ppm. Furthermore, a broad peak at 5.18 ppm assigned to the alcoholic proton in aliphatic moiety exhibited an up field shift by $\Delta\delta = -0.38$ ppm in complex spectrum (Fig. S5b). These findings proposed that the imine nitrogen ($\text{CH}=\text{N}$) and OH groups of receptor **L** participated to complex zinc ions. Hence, it is noticeable that Zn^{2+} ions coordinated to the receptor via deprotonation of the phenol and the chelation with the imino nitrogen, and not from the azo group chelated to the thiazole S atom (or N via an E/Z isomerization). Hence, the recognition mechanism of sensor **L** for Zn^{2+} can be obtained by combining the Job's plot, molar ratio plot, MALDI-TOF mass and FT-IR results. Consequently, we proposed the formation of 2:1 complex as shown in Scheme 2.

Reversibility is an important concept in chemistry which has an aptitude to recover free receptor from the complex. To inspect the reversible interaction of receptor **L** toward Zn^{2+} in DMSO, Ethylenediaminetetraacetic acid (EDTA) solution (10 equivalent) was added to the complex solution of receptor **L** ($5 \times 10^{-5}\text{ M}$) and Zn^{2+} (10 equivalent) (Sheng et al. 2008; Gupta et al. 2013). As expected, the absorbance intensity almost decreased to the absorbance intensity of free receptor as shown in Fig. S6. Also, the primary color of the probe was recovered instantly. These

Fig. 1 a Color changes of **L** in DMSO (4×10^{-5} M) before and after the addition of 20 equiv. of respective metal ions. **b** Absorption spectra of the receptor **L** recorded in DMSO after addition of 0–20 equiv. of Zn^{2+} ions, (Inset of molar ratio plot)

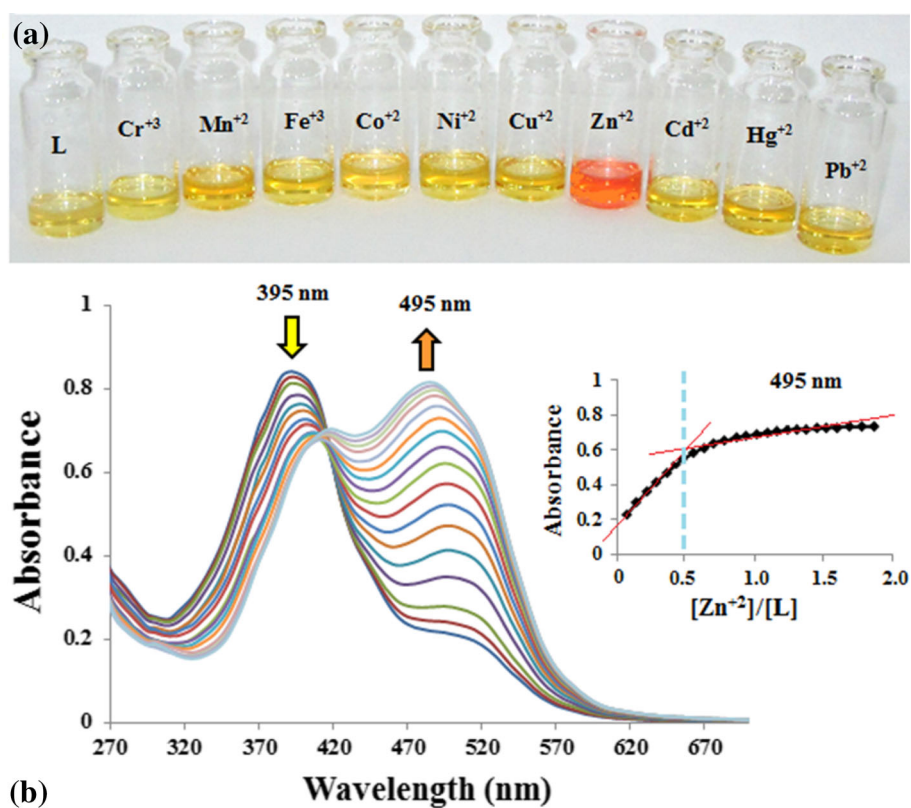
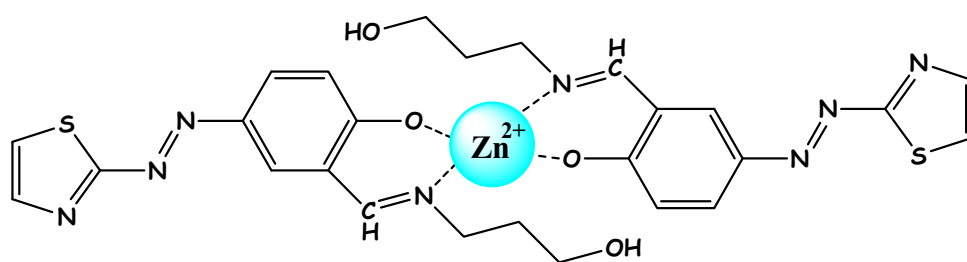


Table 1 Data obtained from the UV–Vis spectra upon titration of receptor **L** (4×10^{-5} M) with Zn^{2+} metal ions in DMSO

Receptor + cation	Receptor, λ_{max} (nm)	Complex, λ_{max} (nm)	ϵ ($\text{M}^{-1} \text{cm}^{-1}$)	Bathochromic shift, $\Delta\lambda_{\text{max}}$ (nm)	Isobestic point, (nm)	K_a (M^{-1})	LOD (μM)
L–Zn²⁺	395	495	233	100	410	1.07×10^9	48.9

Scheme 2 Proposed structure of Zn^{2+} Complex



findings may be attributed to the stronger complexation of Zn^{2+} with EDTA than with sensor **L** (Likussar and Boltz 1971). Hence, compound **L** was a reversible chemosensor for Zn^{2+} ions.

The most important limitations for zinc detection comes from the interference of very pollutant cations such as cadmium and lead. The selectivity towards Zn^{2+} was further clarified by the competitive binding experiment. To perform this, the receptor **L** (4×10^{-5} mol L^{-1}) was

treated with Zn^{2+} in the presence of 10 equiv. of Cd^{2+} and Pb^{2+} ions in DMSO. As illustrated in Fig. S7 Cd^{2+} and Pb^{2+} ions had no interference with the detection of Zn^{2+} at 495 nm. So, the chemosensor **L** has revealed a good practical ability to recognize Zn^{2+} in the presence of Cd^{2+} and Pb^{2+} ions.

Electronic absorption studies of **L** toward different anions

The anion recognition property of the probe **L** was initially investigated on a qualitative basis by visual testing of the anion-induced color changes and then absorption spectral studies in DMSO ($4 \times 10^{-5} \text{ mol L}^{-1}$) before and after the addition of 2 equivalent of typical anions such as F^- , Cl^- , Br^- , I^- , H_2PO_4^- , HSO_4^- , AcO^- and NO_3^- as their tetrabutylammonium (TBA) salts. As shown in Fig. 2a only H_2PO_4^- , F^- and AcO^- ions could induce the sensor to form a clear color change from yellow to red, suggesting strong interaction between the receptors with relatively basic anions, while other anions had no noticeable color changes. Moreover, spectroscopic studies showed that the basic anions like F^- , H_2PO_4^- and AcO^- ions had an extreme effect on the electronic spectra of receptors. However, there were no special changes in the absorption spectra in the presence of other anions, Fig. 2b.

The change in optoelectronic properties of azo-linked salicylaldimine Schiff base ligand in the presence of fluoride, di-hydrogen-phosphate and acetate anions was investigated by UV–Vis spectroscopic method. The titrations were carried out in DMSO at $4.0 \times 10^{-5} \text{ mol L}^{-1}$ concentration of receptor **L** upon the addition of incremental amounts of ($5.0 \times 10^{-4} \text{ mol L}^{-1}$) tetrabutylammonium fluoride, di-hydrogen-phosphate and acetate. As shown in Fig. 3 and Fig. S8, a new red shifted absorption band at 510 nm was progressively enhanced when the concentration of H_2PO_4^- , F^- and AcO^- was increased in the receptor **L**, while the intensity of absorption at 395 nm decreased correspondingly. A clear isosbestic point was observed at 435 nm for complexation of **L** with H_2PO_4^- . The appearance of a single isosbestic point in UV–Vis

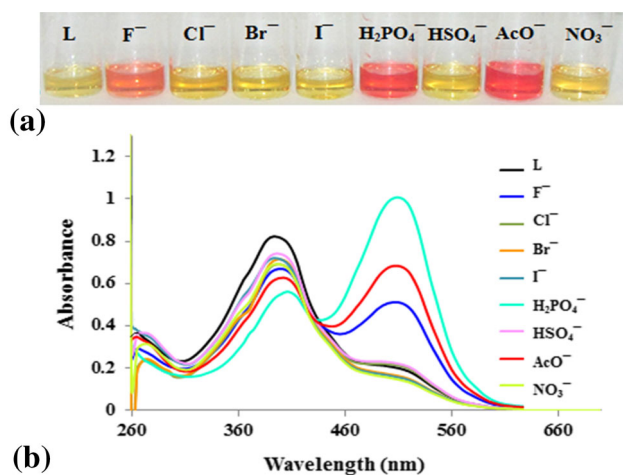


Fig. 2 Color changes (a) and UV–Vis absorption spectra (b) of receptor **L** ($4 \times 10^{-5} \text{ mol L}^{-1}$ in DMSO) in the presence of 2 equiv. of different anions as their TBA salts

spectra of **L** with incremental addition of H_2PO_4^- indicates the presence of only two species, neutral host and its anion in the solution (Arabahmadi et al. 2014). Also, the definite stoichiometric ratio between **L** and H_2PO_4^- anion was determined to be 1:1 from UV–Vis spectral changes with the help of molar ratio plot and Job's plot experiment (inset of Fig. 3) which suggests that receptor **L** interacts with H_2PO_4^- anion as a bidentate ligand. Moreover, noticeable isosbestic points were observed at 435 and 433 nm for complexation of **L** with F^- and AcO^- , respectively. The molar ratio plot and Job's plot analysis of the UV–Vis titrations of **L** revealed a 1:2 binding stoichiometry for F^- and AcO^- anions (inset of Fig. S8a, b). The 1:2 stoichiometry ratio verify that **L** (1 equivalent) interacts with F^- or AcO^- ions (2 equivalents) through both phenolic O–H and alcoholic O–H. Deprotonation of phenolic hydroxyl results in a noticeable isobestic point; however, the taking of aliphatic hydroxyl proton is not captured in the UV–Vis spectrum given the great isobestic point, because the alcoholic proton is not in a conjugated system so would potentially not lead to a spectroscopic change. Nevertheless, the obtained results demonstrated the Hydrogen bond interactions between the host and the anionic guests affecting the electronic properties of the chromophore (Benesi and Hildebrand 1949).

Furthermore, the molar absorption coefficient (ϵ) for H_2PO_4^- , F^- and AcO^- complexes of **L** were obtained as 32,275, 16,378 and 21,891 ($\text{M}^{-1} \text{ cm}^{-1}$), respectively. These results show that hydrogen bonding formed by H_2PO_4^- is stronger than hydrogen bonding formed in F^- and AcO^- complexes of **L**. It has been reported in previous literatures that multiple hydrogen bonding interactions are necessary in high-affinity anion binding sites. Charge and shape complementarity between the host and anionic guests are also extremely important (Arabahmadi et al.

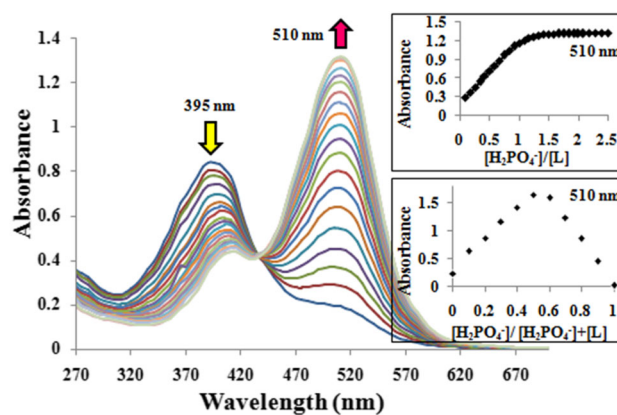


Fig. 3 UV–Vis titration of **L** ($4 \times 10^{-5} \text{ mol L}^{-1}$) in DMSO with incremental addition of H_2PO_4^- anions as its TBA salt (0–2 equiv.). Insets showing the molar ratio plot (top) and job plot (bottom) at selected wavelength

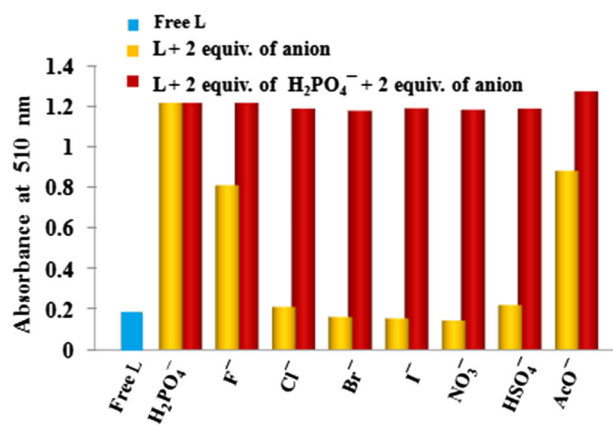
Table 2 Data obtained from the UV–Vis spectra upon titration of receptor **L** with TBAH₂PO₄, TBAF and TBAOAc in DMSO

Receptor + ion	Receptor, λ_{\max} (nm)	Complex, λ_{\max} (nm)	ϵ (M ⁻¹ cm ⁻¹)	Bathochromic shift, $\Delta\lambda_{\max}$ (nm)	Isobestic point, (nm)	K_a (M ⁻¹)	LOD (M)
L–H ₂ PO ₄ ⁻	395	510	32,275	115	435	1.027×10^5	3.24×10^{-6}
L–F ⁻	395	510	16,378	115	435	3.710×10^4	2.91×10^{-7}
L–AcO ⁻	395	510	21,891	115	433	1.020×10^4	3.01×10^{-7}

2014). The resulting values are summarized in Table 2. The binding constant of complexation was calculated using the Benesi–Hildebrand method. The Benesi–Hildebrand plot of $1/[A-A_0]$ versus $1/[ion]$ for titration of **L** with H₂PO₄⁻, F⁻ and AcO⁻ produced a straight line (Fig. S9). Receptor **L** complexes binding constants for H₂PO₄⁻, F⁻ and AcO⁻ were obtained from the variation in the absorbance at 510 nm. Moreover, the binding constants and the detection limits of the sensor **L** towards corresponding anions were obtained from UV–Vis titration, as listed in Table 2.

For practical applications, further UV–Vis spectrophotometric titrations in aqueous media were carried out for the sensor **L** (4×10^{-5} mol L⁻¹) in 9:1 DMSO/H₂O solutions upon addition of F⁻, H₂PO₄⁻ and AcO⁻ as their inorganic sodium salt in water. It is noticeable that titration of **L** with NaH₂PO₄, NaF and NaAcO produced similar color and spectral changes to that described in organic media (Fig. S10a–c). Moreover, the job plots of **L** with H₂PO₄⁻, F⁻ and AcO⁻ were established to be 1:1, 1:2 and 1:2 stoichiometric ratios from UV–Vis spectral changes, respectively, confirming that the interaction stoichiometry between receptor and anion was not affected by the presence of competitive water molecules (Fig. S11).

The absorbance enhancement of sensor **L** with H₂PO₄⁻ was investigated in the presence of other anions at 510 nm to examine the selectivity for H₂PO₄⁻ in a complex background of potentially competing species. To accomplish this, the sensor **L** (4×10^{-5} mol L⁻¹) was treated with 2 equivalent of H₂PO₄⁻ in the presence of other competing anions in the same concentration. As illustrated in Fig. 4 sensor **L** exhibited maximum absorbance for H₂PO₄⁻ between other anions at 510 nm in DMSO (yellow columns). Moreover, a background of other competing anions did not interfere with the detection of H₂PO₄⁻ by **L** in DMSO (red columns). These results indicate that **L** exhibits good selectivity for H₂PO₄⁻ over competing relevant anions. Since the receptor **L** senses both Zn²⁺ metal ions and F⁻, AcO⁻ and H₂PO₄⁻ anions, we examined the effect of sensing ability in the presence of competing ions. So, the receptor was treated with 2 equivalents of anions in the presence of Zn²⁺ ions (Fig. S12). It is obvious that **L** has different manner of binding anions.

**Fig. 4** Behavior of receptor **L** toward H₂PO₄⁻ and other anions as measured by UV–Vis in DMSO at 510 nm

Upon addition of H₂PO₄⁻ into the mixture of **L** and Zn²⁺, the primary color and absorption spectra of the probe were recovered. These findings may be attributed to the stronger complexation of Zn²⁺ with H₂PO₄⁻ than with sensor **L**. While, addition of F⁻ and AcO⁻ into the mixture of **L**–Zn²⁺ complex caused no clear change in color or their absorption spectra.

On the other hand, as a probe for the assigned anion, response time is of importance to practical detection of analytes. The effect of the reaction time on the binding process of F⁻, H₂PO₄⁻ and AcO⁻ to receptor **L** was investigated (Fig. S13). After 36 h, there was a slight or no significant change in the absorption spectrum, which suggests that the sensor **L** is very suitable probe for practical purposes in a long time.

¹H-NMR titration

To further clarify the binding interaction of receptor **L** with F⁻, ¹H-NMR titration experiments were carried out in DMSO-d₆ (Fig. 5). Before the addition of anion, in ¹H-NMR spectra of the receptor, the two singlet resonances in the 11.61 and 9.36 ppm region could be attributed to phenol and imine proton, respectively. After the addition of two equivalents of fluoride ions, the resonance at 11.61 ppm corresponding to phenolic proton disappeared,

Fig. 5 $^1\text{H-NMR}$ titration plot of sensor (**L**) with F^- in $\text{DMSO-}d_6$ (expand of aromatic region)

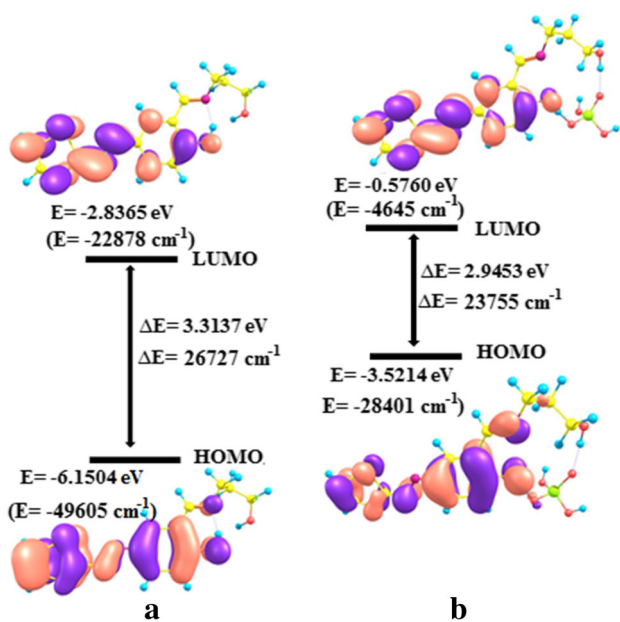
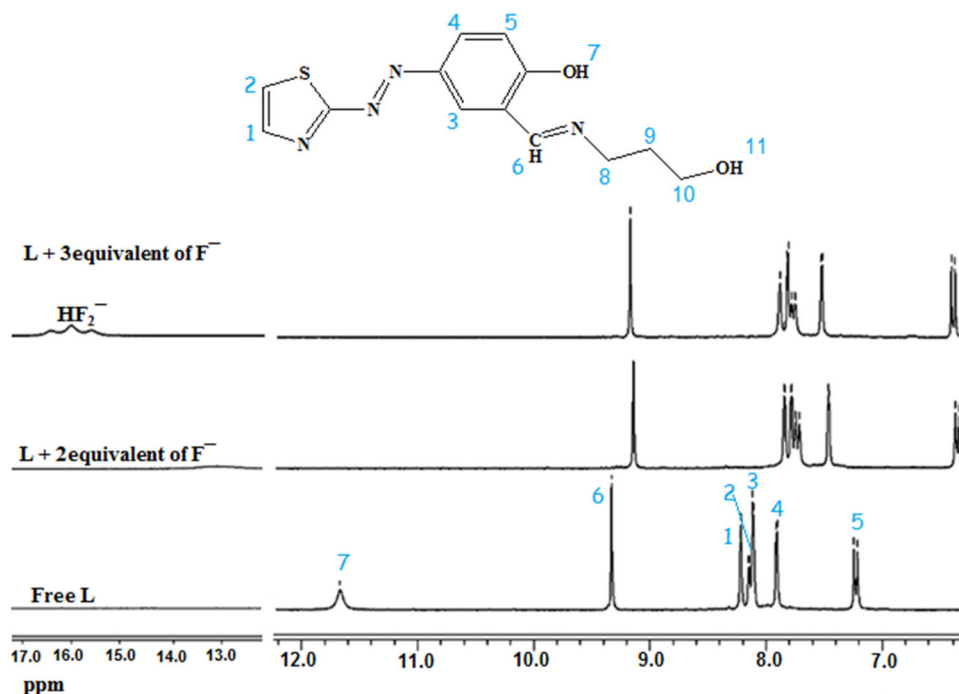


Fig. 6 Energy level diagrams of the HOMO and LUMO orbital of **a** **L** and **b** $\text{L-H}_2\text{PO}_4^-$ complex (using the DFT/B3LYP/6-311++G(d,p) method)

which suggested that the O–H groups underwent a deprotonation process. The aromatic protons shifted up field, which suggests that the negative charges developed from deprotonation of **L** by F^- were delocalized through the whole receptor molecule (Park et al. 2012). In addition, a broad peak at 5.18 ppm in the free receptor was attributed to the disappearance of alcoholic OH due to deprotonation

Table 3 Computational optimized Energy (a.u.) of free receptor **L** and $[\text{L-H}_2\text{PO}_4^-]$ complex in gas phase and in DMSO solvent

Phase	Receptor L	$[\text{L-H}_2\text{PO}_4^-]$ complex
Gas phase	– 1271.6654	– 1915.4588
Solvent (DMSO)	– 1271.6936	– 1915.5410

with F^- . As expected, several new resonances appeared in the aliphatic region at 1–4 ppm upon the addition of TBAF to the solution of receptor, which corresponds to the protons of tetrabutylammonium salt (see supplementary data, Fig. S14). With continuous addition of fluoride ions, a new signal appeared at $\delta = 16.12$ ppm, which indicated the formation of HF_2^- in the $^1\text{H-NMR}$ spectra (Likussar and Boltz 1971; Arabahmadi and Amani 2013, 2014). Hence, we suggested that the F^- recognition occurred due to the initial hydrogen bonding of the anion to the receptor, followed by deprotonation that brought electron density onto the π -conjugated framework through bond propagation, thereby causing a shielding effect and inducing up field shift of aromatic protons (Orojloo and Amani 2016).

Moreover, to confirm the mechanism, we investigated the interaction of receptor **L** in $\text{DMSO-}d_6$ with acetate anion as its sodium salt in D_2O . To perform this, one equivalent of AcO^- anion was added to the solution of **L**, and the spectrum underwent a considerable changes. The peak at 11.61 ppm corresponding to the proton of phenolic OH disappeared. This demonstrates the interaction of anion through the phenolic OH is more effective than interaction through the alcoholic OH groups present in the receptor.

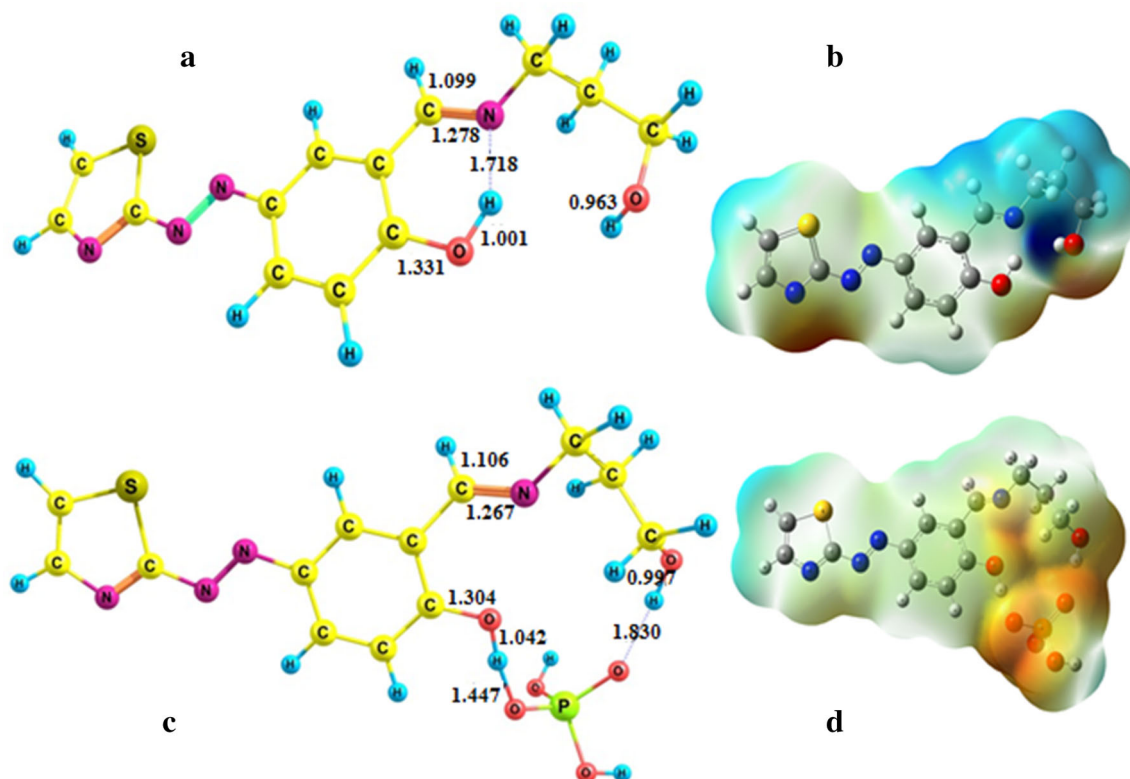


Fig. 7 **a** optimized structure of **L**, **b** MEP map diagram of **L**, **c** optimized structure of **L:H₂PO₄⁻** complex and **d** MEP map diagram of **L:H₂PO₄⁻** complex, by B3LYP/6-311++G(d,p)

The aromatic protons shifted up field, because negative charges developed from deprotonation of **L** by AcO^- ions were delocalized via the whole receptor molecule (Park et al. 2012). Also, deprotonation of the alcoholic hydroxyl of the receptor can occur by addition of two equivalents of AcO^- ions, as is shown in Fig. S15.

Computational studies

In a bid to back up the experimental work, quantum chemical calculations were carried out using Gaussian03 program package (Frisch et al. 2004). Molecular geometry optimizations of the receptor **L** and [**L**- H_2PO_4^-] complex were obtained by density functional theory (DFT) employing the 6-311++G(d,p) basis set. Quantum chemical calculation and molecular studies helped to forecast the electronic structure properties, energy of optimized structures and the probable mode of binding of Ligand **L** with the guest ion H_2PO_4^- . To have a better understanding of the response mechanism of receptor **L**, the representative transition energy diagram for the Highest Occupied Molecular Orbital (HOMO) and the Lowest Unoccupied Molecular Orbital (LUMO) of the receptor-Ligand [**L**- H_2PO_4^-]-complex were obtained, which is shown in Fig. 6. The complexation of **L** with H_2PO_4^- distorted the electron

density distribution of the receptor due to the formation of hydrogen bonds. HOMO's for **L** were localized mainly on the O-H of phenolic moiety and nitrogen of imine group whereas, LUMO was distributed only on the phenolic moiety of the receptor **L**. As a result, hydrogen bond is formed between phenolic O-H and imine group. Conversely, the electron density distribution changed for both receptor moieties and H_2PO_4^- of the complex. One of the hydrogen bond was formed between phenolic O-H and oxygen atom of H_2PO_4^- group. The second hydrogen bond was formed between alcoholic O-H and oxygen atom of H_2PO_4^- anion. The total energy of the optimized complex (-1915.4588 a.u.) in the gas phase was lower compared to the energy of the receptor (-1271.6654 a.u.) thereby protecting the greater stability of the complex (Table 3). Theoretical calculations also revealed the lowest orbital energy gap of [**L**- H_2PO_4^-] complex ($\Delta E = 2.9453$ eV) which is lower than that of free receptor **L** ($\Delta E = 3.3137$ eV). The red-shift phenomenon of the UV-Vis absorption spectra may result from the decrease in energy gap of HOMO and LUMO on complexation with H_2PO_4^- (Fig. 3) (Orojloo and Amani 2017). Calculation of optimized energy of the free **L** and [**L**- H_2PO_4^-] complex in DMSO solvent was also carried out. The results of the calculation in gas phase and solution phase are in agreement with each other (Table 3).

Molecular Electrostatic Potential (MEP) diagrams were produced using the surface analysis of suite program. Among the electronic properties of these molecules, the molecular electrostatic potential (MEP) has been chosen to discover those regions where electron rich moieties can interact. The diagrams indicated the most positive regions in deep blue color were located mainly around the OH protons of receptor moieties (Fig. 7b). These blue-colored positive regions around the OH protons stimulated H_2PO_4^- to take part in Hydrogen bonding. The optimized complex structure of **L** plus H_2PO_4^- showed that one H_2PO_4^- anion was attached with two OH parts of **L** to form a stable 1:1 complex (Fig. 7c). At this point, each H_2PO_4^- anion remained with **L** through two hydrogen bonding interactions, where both phenolic and alcoholic hydroxyl groups interacted with two different 'O' atoms of H_2PO_4^- . The intermolecular distances found for the $[\text{L}-\text{H}_2\text{PO}_4^-]$ -complex are 1.447 Å and 1.830 Å, since hydrogen bonds of phenolic and alcoholic O–H of **L** interacted with two oxygen atoms of H_2PO_4^- fragment, respectively.

Conclusion

Conclusively, we have successfully designed and prepared a simple receptor **L** for the detection of selected Zn^{2+} cation and F^- , H_2PO_4^- and AcO^- anions. The highly selective recognition of Zn^{2+} ions resulted in dramatic color change from yellow to orange in the presence of other competing metal ions that was clearly visible to the naked eye. In addition, receptor **L** had higher sensitivity for basic anions by inducing a rapid color change from yellow to red, and is capable of recognizing F^- , H_2PO_4^- and AcO^- anions both in organic and aqueous media. Consequentially, the DFT calculations upheld the chemosensor selectivity by the decrease in the energy gap between HOMO and LUMO. On the basis of the experimental results, we believe that receptor **L** will offer a qualified chemosensor for recognizing both cations and anions and can be used in environmental application which will be of great importance for real-time and instrument-free detection.

Acknowledgements The authors (M. Orojloo and S. Amani) would like to thank the Research Council of Arak University for financial support of this research.

References

- Arabahmadi R, Amani S (2013) Synthesis and studies of selective chemosensors for anions and cations by azo-containing salicylaldehyde-based receptors. *J Coord Chem* 66(2):218–226
- Arabahmadi R, Amani S (2014) A new fluoride ion colorimetric sensor based on azo–azomethine receptors. *Supramol Chem* 26(5–6):321–328
- Arabahmadi R, Orojloo M, Amani S (2014) Azo Schiff bases as colorimetric and fluorescent sensors for recognition of F^- , Cd^{2+} and Hg^{2+} ions. *Anal Methods* 6(18):7384–7393
- Assaf S, Chung S-H (1984) Release of endogenous Zn^{2+} from brain tissue during activity. *Nature* 308(5961):734–736
- Beer PD, Gale PA (2001) Anion recognition and sensing: the state of the art and future perspectives. *Angew Chem Int Ed* 40(3):486–516
- Benesi HA, Hildebrand J (1949) A spectrophotometric investigation of the interaction of iodine with aromatic hydrocarbons. *J Am Chem Soc* 71(8):2703–2707
- Berg JM, Shi Y (1996) The galvanization of biology: a growing appreciation for the roles of zinc. *Science* 271(5252):1081
- Borisenko V et al (2006) Hydrogen bonds of 2-aminothiazoles in intermolecular complexes (1:1 and 1:2) with proton acceptors in solutions. *J Mol Struct* 783(1):101–115
- Borisova NE, Reshetova MD, Ustynuk YA (2007) Metal-free methods in the synthesis of macrocyclic Schiff bases. *Chem Rev* 107(1):46–79
- Buccella D, Horowitz JA, Lippard SJ (2011) Understanding zinc quantification with existing and advanced ditopic fluorescent Zinpyr sensors. *J Am Chem Soc* 133(11):4101–4114
- Burdette SC, Lippard SJ (2001) ICC34—golden edition of coordination chemistry reviews. *Coordination chemistry for the neurosciences*. *Coord Chem Rev* 216:333–361
- Burdette SC, Lippard SJ (2003) Meeting of the minds: metalloneurochemistry. *Proc Natl Acad Sci* 100(7):3605–3610
- Canpolat E, Kaya M (2005) Studies on mononuclear chelates derived from substituted Schiff Base ligands: synthesis and characterization of a new 5-methoxysalicylidene-p-aminoacetophenoneoxime and its complexes with Co (II), Ni (II), Cu (II), and Zn (II). *Russ J Coord Chem* 31(11):790–794
- Chohan ZH et al (2004) Isatin-derived antibacterial and antifungal compounds and their transition metal complexes. *J Enzyme Inhib Med Chem* 19(5):417–423
- Cozzi PG (2004) Metal-Salen Schiff base complexes in catalysis: practical aspects. *Chem Soc Rev* 33(7):410–421
- Falchuk KH (1998) The molecular basis for the role of zinc in developmental biology. In: Pierce GN, Izumi T, Rupp H, Grynberg A (eds) *Molecular and cellular effects of nutrition on disease processes*, vol 26. Springer, Boston
- Frederickson CJ et al (2006) Synaptic release of zinc from brain slices: factors governing release, imaging, and accurate calculation of concentration. *J Neurosci Methods* 154(1):19–29
- Frisch M et al (2004) Gaussian 03, revision C. 02. Gaussian, Inc., Wallingford, p 26
- Gale PA, Garcia-Garrido SE, Garric J (2008) Anion receptors based on organic frameworks: highlights from 2005 and 2006. *Chem Soc Rev* 37(1):151–190
- Gentili PL (2007) Boolean and fuzzy logic implemented at the molecular level. *Chem Phys* 336(1):64–73
- Gunnlaugsson T et al (2006) Anion recognition and sensing in organic and aqueous media using luminescent and colorimetric sensors. *Coord Chem Rev* 250(23):3094–3117
- Gupta VK et al (2013) Comparative study of colorimetric sensors based on newly synthesized Schiff bases. *Sens Actuators B Chem* 182:642–651
- Hu R et al (2010) A rapid aqueous fluoride ion sensor with dual output modes. *Angew Chem Int Ed* 49(29):4915–4918
- Jiang P, Guo Z (2004) Fluorescent detection of zinc in biological systems: recent development on the design of chemosensors and biosensors. *Coord Chem Rev* 248(1):205–229

- Joseyphus RS, Dhanaraj CJ, Nair MS (2006) Synthesis and characterization of some Schiff base transition metal complexes derived from vanillin and L (+) alanine. *Transition Met Chem* 31(6):699–702
- Kang SO et al (2010) Cryptand-like anion receptors. *Chem Soc Rev* 39(10):3980–4003
- Lavigne JJ, Anslyn EV (2001) Sensing a paradigm shift in the field of molecular recognition: from selective to differential receptors. *Angew Chem Int Ed* 40(17):3118–3130
- Lee MH et al (2010) A novel strategy to selectively detect Fe(III) in aqueous media driven by hydrolysis of a rhodamine 6G Schiff base. *Chem Commun* 46(9):1407–1409
- Leung AC, MacLachlan MJ (2007) Poly (salphenyleneethynylene) s: soluble, conjugated metallopolymers that exhibit unique supramolecular crosslinking behavior. *J Mater Chem* 17(19):1923–1932
- Li S-H et al (2009) Enhanced fluorescence sensing of hydroxylated organotins by a boronic acid-linked Schiff base. *Chem Commun* 28:4179–4181
- Li N, Xiang Y, Tong A (2010) Highly sensitive and selective “turn-on” fluorescent chemodosimeter for Cu^{2+} in water via Cu^{2+} -promoted hydrolysis of lactone moiety in coumarin. *Chem Commun* 46(19):3363–3365
- Li H, Lalancette RA, Jäkle F (2011) Turn-on fluorescence response upon anion binding to dimesitylboryl-functionalized quaterthiophene. *Chem Commun* 47(33):9378–9380
- Li J et al (2012) A highly selective and sensitive polymer-based OFF-ON fluorescent sensor for Hg^{2+} detection incorporating salen and perylenyl moieties. *J Mater Chem* 22(2):478–482
- Li Y-P et al (2013) A new ditopic ratiometric receptor for detecting zinc and fluoride ions in living cells. *Analyst* 138(18):5486–5494
- Li Y et al (2014) A bimodal multianalyte simple molecule chemosensor for Mg^{2+} , Zn^{2+} , and Co^{2+} . *Dalton Trans* 43(4):1881–1887
- Likussar W, Boltz D (1971) Theory of continuous variations plots and a new method for spectrophotometric determination of extraction and formation constants. *Anal Chem* 43(10):1265–1272
- Lin H-Y et al (2012) A turn-on and reversible fluorescence sensor for zinc ion. *Analyst* 137(19):4415–4417
- Liu A et al (2013) A novel rhodamine-based colorimetric and fluorescent sensor for the dual-channel detection of Cu^{2+} and Fe^{3+} in aqueous solutions. *Dyes Pigm* 99(2):472–479
- Maret W et al (1999) Inhibitory sites in enzymes: zinc removal and reactivation by thionein. *Proc Natl Acad Sci* 96(5):1936–1940
- Martinez-Manez R, Sancenón F (2003) Fluorogenic and chromogenic chemosensors and reagents for anions. *Chem Rev* 103(11):4419–4476
- Martínez-Mañez R, Sancenón F (2006) Chemodosimeters and 3D inorganic functionalised hosts for the fluoro-chromogenic sensing of anions. *Coord Chem Rev* 250(23):3081–3093
- Modi J, Sabnis S, Deliwala C (1970) Potential anticancer agents. III. Schiff bases from benzaldehyde nitrogen mustards and aminophenylthiazoles. *J Med Chem* 13(5):935–941
- Momoki K et al (1969) Theory of curved molar ratio plots and a new linear plotting method. *Anal Chem* 41(10):1286–1299
- Orojloo M, Amani S (2016) Synthesis and studies of selective chemosensor for naked-eye detection of anions and cations based on a new Schiff-base derivative. *Talanta* 159:292–299
- Orojloo M, Amani S (2017) Naked-eye detection of cyanide ions in aqueous media based on an azo-azomethine chemosensor. *C R Chim* 20(4):415–423
- Orojloo M et al (2017) Synthesis and characterization of cobalt (II), nickel (II), copper (II) and zinc (II) complexes derived from two Schiff base ligands: spectroscopic, thermal, magnetic moment, electrochemical and antimicrobial studies. *Inorg Chim Acta* 467:227–237
- Park S et al (2012) Azo dye-based latent colorimetric chemodosimeter for the selective detection of cyanides in aqueous buffer. *Sens Actuators B Chem* 174:140–144
- Prodi L, Montalti M, Zaccheroni N (2011) Luminescence applied in sensor science, vol 300. Springer Science & Business Media, New York
- Safin DA, Babashkina MG, Garcia Y (2013) Crown ether-containing Schiff base as a highly efficient “turn-on” fluorescent sensor for determination and separation of Zn^{2+} in water. *Dalton Trans* 42(6):1969–1972
- Santos-Figueroa LE et al (2013) Chromogenic and fluorogenic chemosensors and reagents for anions. A comprehensive review of the years 2010–2011. *Chem Soc Rev* 42(8):3489–3613
- Sarkar K et al (2009) Selective zinc (II)-ion fluorescence sensing by a functionalized mesoporous material covalently grafted with a fluorescent chromophore and consequent biological applications. *Adv Func Mater* 19(2):223–234
- Sessler JL, Seidel D (2003) Synthetic expanded porphyrin chemistry. *Angew Chem Int Ed* 42(42):5134–5175
- Shang L, Jin L, Dong S (2009) Sensitive turn-on fluorescent detection of cyanide based on the dissolution of fluorophore functionalized gold nanoparticles. *Chem Commun* 21:3077–3079
- Shen R et al (2008) Anion recognition by a novel zinc (II) xanthone-crown ether complex. *Inorg Chem Commun* 11(3):318–322
- Sheng R et al (2008) Colorimetric test kit for Cu^{2+} detection. *Org Lett* 10(21):5015–5018
- Tomat E, Lippard SJ (2010) Ratiometric and intensity-based zinc sensors built on rhodol and rhodamine platforms. *Inorg Chem* 49(20):9113–9115
- Vashi K, Naik H (2004) Synthesis of novel Schiff base and azetidinone derivatives and their antibacterial activity. *J Chem* 1(5):272–275
- Venugopala K, Jayashree B (2003) Synthesis of carboxamides of 2'-amino-4'-(6-bromo-3-coumarinyl) thiazole as analgesic and anti-inflammatory agents. *Indian J Heterocycl Chem* 12(4):307–310
- Vigato P, Tamburini S, Bertolo L (2007) The development of compartmental macrocyclic Schiff bases and related polyamine derivatives. *Coord Chem Rev* 251(11):1311–1492
- Wang Q-Q, Day VW, Bowman-James K (2011) Tunable, shape-shifting capsule for dicarboxylates. *Chem Sci* 2(9):1735–1738
- Wang S et al (2015) A well-defined alternating copolymer based on a salicylaldehyde Schiff base for highly sensitive zinc (II) detection and pH sensing in aqueous solution. *Polym Chem* 6(7):1127–1136
- Xu Z et al (2009) Zn^{2+} -triggered amide tautomerization produces a highly Zn^{2+} -selective, cell-permeable, and ratiometric fluorescent sensor. *J Am Chem Soc* 132(2):601–610
- Xue L et al (2012) Rational design of a ratiometric and targetable fluorescent probe for imaging lysosomal zinc ions. *Inorg Chem* 51(20):10842–10849
- Yoon J et al (2006) Imidazolium receptors for the recognition of anions. *Chem Soc Rev* 35(4):355–360
- Zalewski PD, Forbes IJ, Betts W (1993) Correlation of apoptosis with change in intracellular labile Zn (II) using zinquin [(2-methyl-8-p-toluenesulphonamido-6-quinolyloxy) acetic acid], a new specific fluorescent probe for Zn (II). *Biochem J* 296(2):403–408
- Zyryanov GV, Palacios MA, Anzenbacher P (2007) Rational design of a fluorescence-turn-on sensor array for phosphates in blood serum. *Angew Chem Int Ed* 46(41):7849–7852